WATER-TUNNEL INVESTIGATION OF GEOMETRY-INDUCED SEPARATION OF A TURBULENT BOUNDARY LAYER

Marco Costantini, Christian Klein, Andrea De Vincenzo, Reinhard Geisler, Jonathan Lemarechal, Daniel Schanz, Andreas Schröder, Tobias Knopp, Cornelia Grabe
Institute of Aerodynamics and Flow Technology
German Aerospace Center (DLR)
Bunsenstrasse 10, D-37073 Göttingen (Germany)
Marco.Costantini@dlr.de

Massimo Miozzi
Institute of Marine Engineering
National Research Council (CNR)
Via di Vallerano 139, I-00128 Rome (Italy)

ABSTRACT

The separation of a turbulent boundary layer developing over a flat plate at nearly-zero pressure gradient was experimentally studied in this work in the Large Watertunnel Braunschweig. The reported measurements were conducted via Temperature-Sensitive Paint and Lagrangian Particle Tracking by Shake-The-Box in the region downstream of a backward-facing ramp, which induced a turbulent separation bubble. The examined Reynolds numbers, based on the ramp location, were in the range 1.2 to 2.7 million.

INTRODUCTION

The understanding and prediction of turbulent separated flows are crucial in a variety of aerodynamic applications, and especially at the borders of the flight envelope (e.g., at low-speed/high-lift conditions). Even for the case of flow reattachment after turbulent separation (Turbulent Separation Bubble, TSB), an improvement in the turbulence modeling is still needed in Reynolds-Averaged Navier-Stokes (RANS) equations for the correct prediction of the TSB shape and size (Eisfeld, 2022; Grabe, 2022), but validation efforts based on reference test cases (such as that from Greenblatt et al., 2006) led to contradictive conclusions. For this reason, a new set of experiments was designed and performed within the DLR project *ADaMant* (Grabe, 2022, Costantini et al., 2023). The measurements focused on the investigation of geometry-induced TSB at nearly-zero pressure gradient via 2D and 3D Lagrangian Particle Tracking by Shake-The-Box (STB) (see, e.g., Schröder & Schanz, 2023, and Schanz et al., 2024) and via Temperature-Sensitive Paint (TSP) (see Liu et al., 2021, and Miozzi & Costantini, 2021, among others). STB and TSP are capable to provide the information on the average and instantaneous TSB characteristics necessary for reliable turbulence model validation and modeling extensions (Eisfeld, 2022). A TSB induced by a 25° Backward-Facing Ramp (BFR) was examined in the present work. This BFR configuration was selected since it did not lead to a secondary recirculation within the TSB, as shown in a preceding wind-tunnel experiment (Costantini et al., 2023).

EXPERIMENTAL SETUP

The experiments were performed in the Large Watertunnel (GWB) of the Technical University of Braunschweig. It is a closed-circuit facility with test-section dimensions of 6 × 1 × 1 m^3 (length × width × height). The maximal freestream velocity achievable in the test section is U_∞ = 6 m/s. The measurements were conducted on a flat-plate model, as sketched in Figure 1. The aforementioned 25° BFR was installed at the streamwise location x_h = 1.134 m and had a height h = 8 mm. In analogy with the preceding wind-tunnel experiment (Costantini et al., 2023), the design aimed to achieve a ratio $h/\delta_{99} \sim 0.4$ at x_h, where δ_{99} is the boundary-layer thickness at the ramp location, but in the absence of the BFR. The flat plate was mounted vertically in the test section and spanned the whole test-section height, as shown in Figure 2. The experimental configuration was designed with a main body and exchangeable modules for the installation of different measurement techniques.

For the experiments reported in this work, two modules were used in separate test campaigns: a module for the TSP measurements (*TSP module*), installed in the model picture shown in Figure 2 (left), where the TSP appears as yellow coating; and a module for the STB measurements (*STB module*), sketched in Figure 2 (right) as dark red area, with a glass insert shown as cyan component. The TSP module was composed of two laminates, each of which was coated with a TSP layer consisting of a europium complex (luminophore) incorporated into a commercial polyurethane clear-coat binder (see, e.g., Miozzi & Costantini, 2021, and Miozzi et al., 2024, for a similar TSP formulation). The TSP laminates were embedded into an anodized aluminium frame, which comprised also the BFR. This latter was designed as metallic component in order to guarantee the achievement of the required geometry, and in particular the sharpness of the BFR corners. One laminate was placed upstream of the BFR, with the other one downstream of the BFR, thus covering a streamwise extent of approx. 210 and 240 mm upstream and downstream of the BFR, respectively. The two laminates were manufactured of fiber-reinforced plastic, designed in a manner similar to that presented, e.g., in Costantini et al. (2021) and Miozzi et al. (2024). In particular, a current-carrying carbon fiber layer (CFRP) of 0.1 mm thickness was integrated into each laminate; during the experiments, the CFRP layer was used as electrical heating to increase the temperature distribution on the TSP surfaces above the adiabatic-wall conditions, and thus enhance the flow-induced thermal

signatures. The span width of the TSP laminates was 600 mm, being the effective TSP surfaces 500 mm wide because of the electrical contacting strips placed below their spanwise ends. The STB module was composed of a glass insert embedded into an anodized aluminium frame. The glass insert, designed to avoid light reflection at the wall, had a span width of 150 mm and a streamwise extent of 250 mm. The BFR was directly manufactured into the glass by using a triangle prism and a refractive index matched glue.

The optical measurement system (camera and light sources) for the TSP measurements and the cameras for the STB measurements were mounted in front of circular windows installed in a side-wall panel of the GWB test section (not visible/shown in Figure 2). The high-speed cameras used in the two test campaigns were CMOS Phantom v2640 cameras with a 12-bit dynamic range and a 2048 × 1952 pixels image sensor. As sketched in Figure 2 (right), 5 cameras were used for the STB measurements, thus enhancing the triangulation accuracy. All cameras pointed at the same measurement volume and enabled the acquisition of STB data in a volume of approx. 80 × 90 × 15 mm^3 (streamwise × spanwise × wall-normal) downstream of the BFR. The spatial resolution was increased via a two-stage scanning process, in which the cameras recorded the upper and lower parts of the volume within every even and odd frame, respectively. This was accomplished using a Photonics Industries DM200 Dual Head Nd:YAG laser (532 nm wavelength). The system's two laser beams were separated and guided via individual systems of lenses and mirrors through a circular window in the test-section bottom wall, thus illuminating the upper and lower subvolumes, respectively (Figure 2, right). The cameras recorded at repetition rates of up to 15 kHz (7.5 kHz per subvolume). All cameras for the STB measurements were equipped with 100 mm focal length lenses, and Scheimpflug adapters were employed for the four cameras with axes non-perpendicular to the measurement volume. The particles used in the STB measurements were spherical polyamide particles with an average diameter of 20 µm. Scanning STB processing was carried out as introduced in Schanz et al. (2024).

For the TSP measurements, only the central camera was used, and it was equipped with a lens of 35 mm focal length that enabled capturing a region of approx. 155 × 285 mm^2 (streamwise × spanwise) downstream of the BFR. A band-pass optical filter for the wavelength range of 590–670 nm was installed in front of the lens to capture only the light emitted by the TSP. The camera acquisition frequency for the TSP measurements was 1 kHz. Three in-house, high-power LED systems, with central excitation wavelength of 395 nm, were used for the excitation of the TSP. They were equipped with band-pass filters for the wavelength range 350–420 nm, and were also mounted in front of the circular windows in the test-section side wall.

RESULTS

The measurements were performed at four different freestream velocities (approx. U_∞ = 1.2–2.6 m/s) to achieve Reynolds numbers based on the BFR location in the range $Re_{xh} = 1.2–2.7 \cdot 10^6$, matching those examined in the preceding wind-tunnel experiment (Costantini et al., 2023). In Figure 3, the results obtained at the lowest Reynolds number ($Re_{xh} = 1.2 \cdot 10^6$) are exemplarily shown. An instantaneous map (snapshot) of surface temperature fluctuations (i.e., the difference between the maps of instantaneous temperature and the time-averaged map of the data series) is presented in Figure 3 (left) for the TSP field downstream of the BFR, with the flow from the left. The TSP data analysis showed two different patterns of traces of wall temperature fluctuations: one in the region close to the BFR up to approx. $X = x - x_h = 40$ mm, and the other one further downstream. The different patterns were due to the different boundary-layer states: the flow was separated up to $X \sim 40$ mm, and attached further downstream. These observations were confirmed by the STB results, as shown in Figure 3 (right). In the bottom-right figure, the time- and spanwise-averaged distribution of the streamwise velocity component, with super-imposed streamlines, shows a TSB with the location of flow reattachment in excellent agreement with that found in the TSP results. In the top-right figure, the instantaneous particle tracks close to the surface show a streaky pattern with a similar appearance as that seen in the surface temperature map in Figure 3 (left).

The final contribution will provide a detailed analysis of the experimental data, including the extraction of skin-friction distributions from the time-resolved surface temperature maps via the methodology presented, e.g., in Miozzi & Costantini (2021) and Costantini et al. (2021), and a quantitative comparison between TSP and STB results, such as that reported in Miozzi et al. (2024).

REFERENCES

Costantini, M., Henne, U., Klein, C., Miozzi, M. (2021) Skin-Friction-Based Identification of Critical Lines in Transonic, High Reynolds Number Flow via Temperature-Sensitive Paint. *Sensors* 21(15): 5106.

Costantini, M., Schanz, D., Geisler, R., Schröder, A., Knopp, T., Dormoy, C., Grabe, C., Miozzi. M. (2023) Experimental and numerical study of geometry-induced separation of a turbulent boundary layer. *DLRK 2023*, Stuttgart, Germany, 19–21 Sept. 2023.

Eisfeld, B. (2022) The importance of turbulent equilibrium for Reynolds-stress modeling. *Physics of Fluids* 34: 025123.

Grabe, C. (2022) DLR-Project ADaMant: Adaptive, Data-driven Physical Modeling towards Border of Envelope Applications. *DLRK 2022*, Dresden, Germany, 27-29 Sept. 2022.

Greenblatt, D., Paschal, K. B., Yao, C.-S., Harris, J., Schaeffler, N. W., Washburn, A. E. (2006) Experimental Investigation of Separation Control Part 1: Baseline and Steady Suction, *AIAA Journal* 44(12): 2820-2830.

Liu, T., Sullivan, J. P., Asai, K., Klein, C., Egami, Y. (2021) *Pressure and Temperature Sensitive Paints*, 2nd ed. Springer, Cham, Switzerland.

Miozzi, M., Costantini, M. (2021) Temperature and skin-friction maps on a lifting hydrofoil in a propeller wake. *Measurement Science and Technology* 32(11): 114007.

Miozzi, M., Schröder, A., Schanz, D., Willert, C. E., Klein, C., Lemarechal, J. (2024) Skin friction from temperature and velocity data around a wall mounted cube. *Experiments in Fluids* 65: 156.

Schanz, D., Schröder, A., Bosbach, J., Strübing, T., Wolf, C. C., Schwarz, C., Heintz, A. (2024) Scanning Lagrangian particle tracking to measure 3D large scale aerodynamics of quadcopter flight. *21st International Symposium on Applications of Laser and Imaging Techniques to Fluid Mechanics*, Lisbon, Portugal, 8-11 July 2024.

Schröder, A., Schanz, D. (2023) 3D Lagrangian Particle Tracking in Fluid Mechanics. *Annual Review of Fluid Mechanics* 55: 511-540.

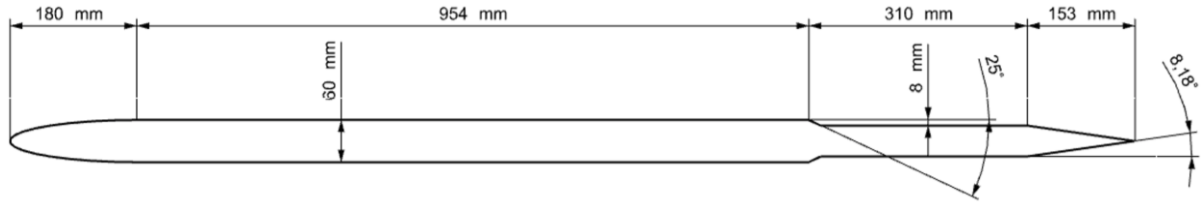

Figure 1. Sketch of the flat-plate model with 25° backward-facing ramp (side view).

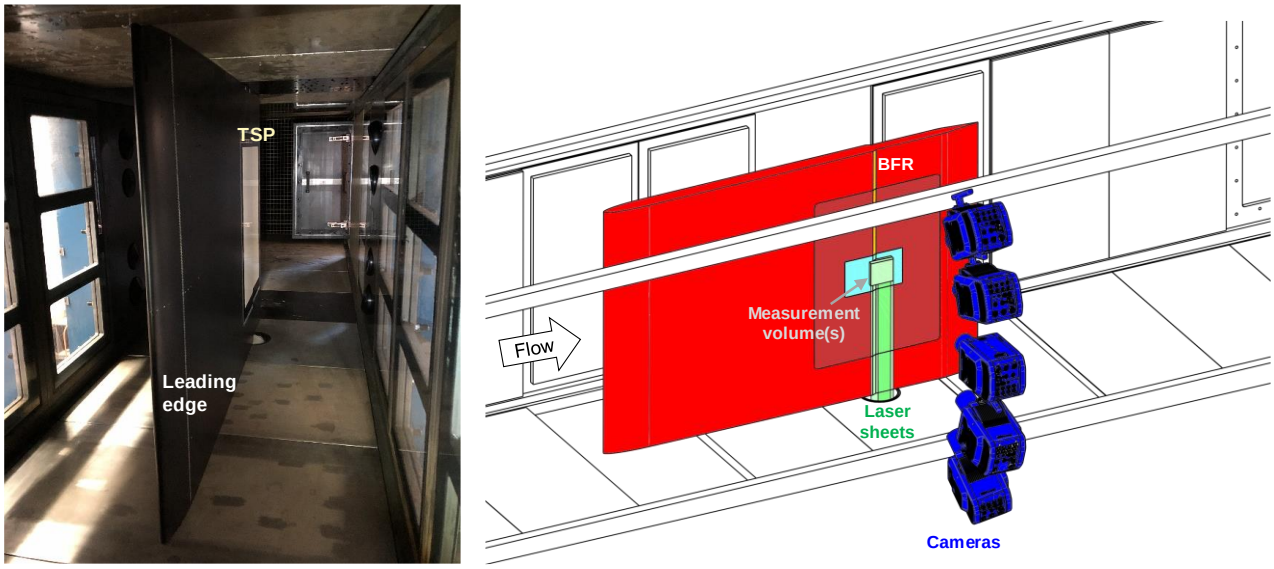

Figure 2. Left: flat-plate model with TSP module installed in the GWB test section. View in the flow direction. Right: sketch of the experimental setup for the STB measurements: flat-plate model (red), STB module with glass insert (dark red and cyan, respectively), 5 high-speed cameras (blue) and laser sheets (green).

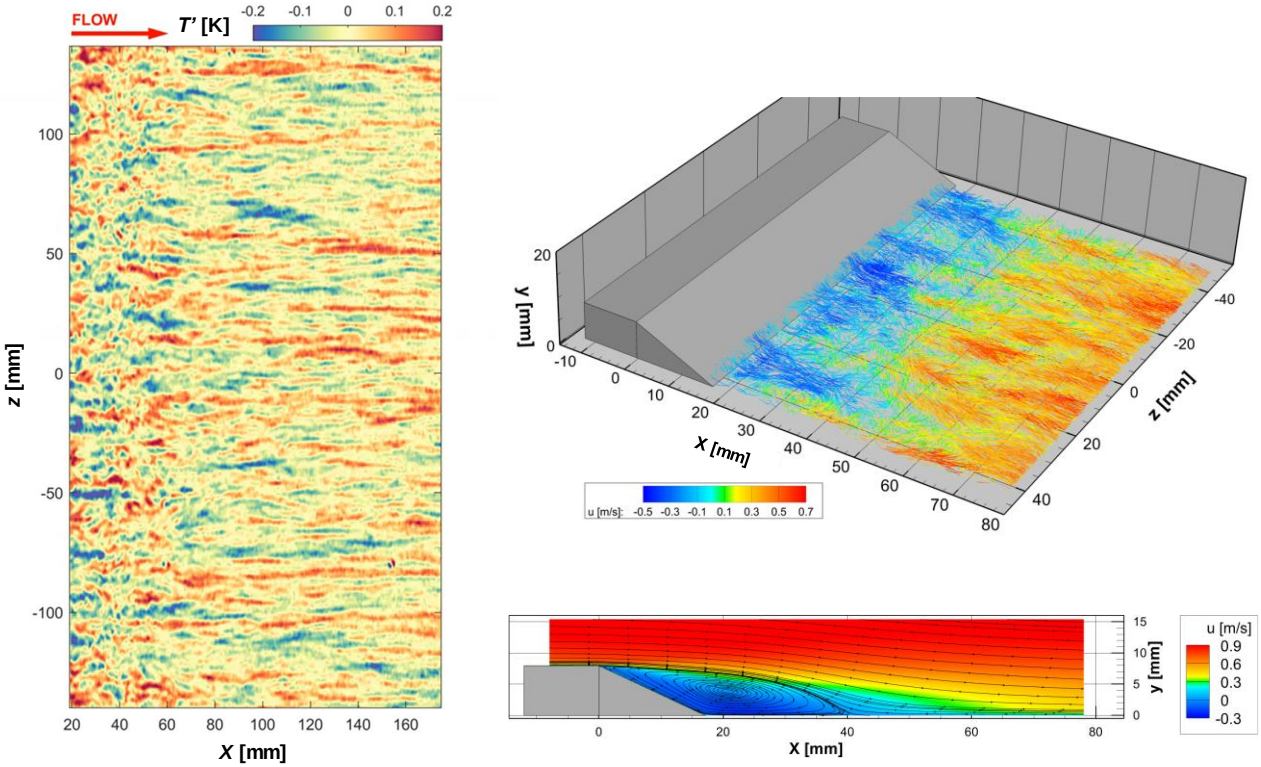

Figure 3. TSP (left) and STB results (right) at $Re_{xh} = 1.2 \cdot 10^6$. $X = 0$ corresponds to the BFR location x_h, $y = 0$ to the vertical location of the plate surface downstream of the BFR, and $z = 0$ to the mid-span location. Left: instantaneous distribution of the surface temperature (snapshot of the temperature fluctuations) on the TSP field downstream of the BFR. Flow from the left. Top, right: instantaneous particle tracks in the vicinity of the surface downstream of the BFR, color-coded by the streamwise-component of the velocity u. Bottom, right: time- and spanwise-averaged u-distribution, with super-imposed streamlines.